

**Demonstration of a new
indicator for studying
upwelling in the northern
South China Sea***

doi:10.5697/oc.53-2.605
OCEANOLOGIA, 53 (2), 2011.
pp. 605–622.

© 2011, by Institute of
Oceanology PAS.

KEYWORDS

Multivariate
statistical analysis
Remote sensing
Upwelling
Silicate
South China Sea

LI LIN^{1,2}, YOU-SHAO WANG^{1,2,3,*}
CUI-CI SUN^{1,2}, NAN LI^{1,2}
HAILI WANG³
B. GREG MITCHELL³
MEI-LIN WU^{1,2}
HUI SONG^{1,2}
JING-FENG WU⁴

¹ State Key Laboratory of Oceanography in the Tropics,
South China Sea Institute of Oceanology,
Chinese Academy of Sciences,
Guangzhou 510301, China;

e-mail address: yswang@scsio.ac.cn

*corresponding author

² Marine Biology Research Station at Daya Bay,
Chinese Academy of Sciences,
Shenzhen 518121, China

³ Scripps Institution of Oceanography,
University of California,
San Diego, CA 92093–0218, USA

⁴ Rosenstiel School of Marine and Atmospheric Science,
University of Miami,
4600 Rickenbacker Causeway, Miami, FL 33149, USA

* This research was supported by the projects of knowledge innovation program of the Chinese Academy of Sciences (No. KZCX2-YW-Q07-02, No. KSCX2-SW-132 and No. KSCX2-YW-Z-1024), the National Natural Science Foundation of China (41076070) and the National 908 project (No. 908-02-04-04).

The complete text of the paper is available at <http://www.iopan.gda.pl/oceanologia/>

Abstract

In order to demonstrate that silicate ($\text{SiO}_3\text{-Si}$) can be used as an indicator to study upwelling in the northern South China Sea, hierarchical cluster analysis (CA) and principle component analysis (PCA) were applied to analyse the metrics of the data consisting of 14 physical-chemical-biological parameters at 32 stations. CA categorized the 32 stations into two groups (low and high nutrient groups). PCA was applied to identify five Principal Components (PCs) explaining 78.65% of the total variance of the original data. PCA found important factors that can describe nutrient sources in estuarine, upwelling, and non-upwelling areas. PC4, representing the upwelling source, is strongly correlated to $\text{SiO}_3\text{-Si}$. The spatial distribution of silicate from the surface to 200 m depth clearly showed the upwelling regions, which is also supported by satellite observations of sea surface temperature.

1. Introduction

Coastal upwelling is an important marine process that has been studied worldwide because of its significant impacts on biogeochemical cycles, primary productivity and fisheries (Prego et al. 2007, Woodson et al. 2007). The process can re-fertilize the surface water with high levels of nutrient by uplifting nutrient-rich subsurface water and thus increase the growth of marine phytoplankton in the surface layer (Shen & Shi 2006, Prego et al. 2007). There are several famous coastal upwelling systems in the world: the Benguela Current (Monteiro & Largier 1999), the California Current (di Lorenzo 2003), the Peru-Chile Current (Nixon & Thomas 2001, Mohtadi et al. 2005) and the Canary Current (Pelegri et al. 2005). These upwelling systems are produced by the interaction between favourable winds and the topography (Woodson et al. 2007), often involving offshore Ekman transport or surface currents.

The upwelling systems in the northern part of the South China Sea (SCS) are still not well understood by marine scientists because of the influence of the Kuroshio Current (KC) passing through the Luzon Strait in the deeper layer (Su & Wang 1990, Hu & Liu 1992, Huang et al. 1992, Chen & Huang 1996), the complex topography (Morton & Blackmore 2000) and the dynamic climatology. There are four coastal upwelling regions in the northern part of the SCS: the east of Guangdong Province and Hainan Province (Han 1998, Wang et al. 2006, 2008, 2011), the Taiwan Shoals (TSLs) located southwest of Taiwan (Wu & Li 2003), and the perennial cold cyclonic eddy (Wu 1991, Huang et al. 1992; Soong et al. 1995, Liao et al. 2006) to the south-west of the Dongsha Islands (PIS).

In the past, the DO concentration, sea surface temperature, salinity and Chl *a* concentration (Chen & Ruan 1991, Hong & Li 1991, Han 1998, Tang et al. 2002) were the main proxies indicating upwelling regions. It is well-known that upwelling always accompanies high nutrient levels (Shen & Shi 2006), but there are relatively fewer reports of upwelling based on nutrient distributions, probably because of their strong relationship with phytoplankton uptake (Traganza et al. 1980, Chen et al. 2004).

Multivariate statistical techniques have been applied to characterize and evaluate surface and freshwater quality, and are useful for verifying the temporal and spatial variations caused by natural and anthropogenic factors linked to seasonality (Helena et al. 2000, Singh et al. 2004, Shrestha & Kazama 2007). In this paper, we attempt to demonstrate the significance of silicate as a useful indicator for the formation and distribution of upwelling events in the northern SCS with multivariate statistical analysis and remote sensing techniques.

2. Material and methods

2.1. Study area

The SCS is located almost exactly between the Equator and the Tropic of Cancer at 22°N (Figure 1), and includes the Pearl River, the third biggest river in China. It thus experiences a monsoon climate. The study area lies

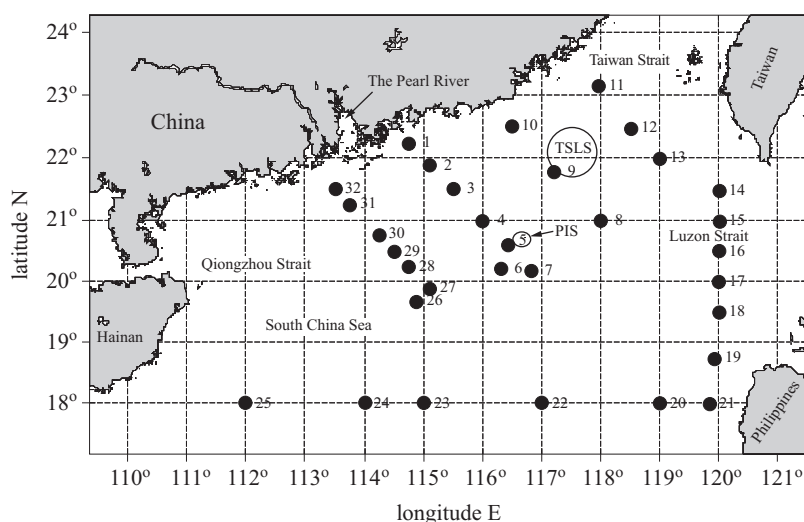


Figure 1. Map of the monitoring stations in the northern SCS. TSLS: Taiwan Shoals; PIS: Dongsha Islands

in the northern SCS (from 18 to 23°N, 111 to 121°E); it is surrounded by several modern cities (Guangzhou, Shenzhen, Hong Kong, Macao) and three straits (the Taiwan Strait (in the north-east), the Luzon Strait (between the islands of Taiwan and Luzon, which connects the SCS with the Pacific Ocean) and the Qiongzhou Strait (in the west)). In the centre of our study area, there is an island called Dongsha (PIS: 116.825°N, 20.691°E), which is the largest island in the SCS. The TSLs are in the south-west of the Taiwan Strait.

The study area is located in a region with a monsoon climate. The strong north-east monsoon prevails during late September–April, and the south-west monsoon during May–August (Chen et al. 2006). The transition from the summer monsoon to the winter monsoon occurs in September.

The following stations were designated to study the formation and distribution of upwelling near the PIS:

1. Stations 1, 2, 3, 32, 31 and 30 near the Pearl River for evaluating the level of nutrients discharged from the river and for eliminating anthropogenic influence.
2. Stations 9, 10, 11, 12 and 13, located in the area of the Taiwan Shoals Upwelling and the East Guangdong upwelling (Han 1998, Shen & Shi 2006, Wang et al. 2006, 2008, 2011).
3. Stations 4, 5, 6, 7, 8, 29, 28 and 27 lie in the area of the PIS, and the left side of this area for detecting the upwelling distribution in this area.
4. Stations 21, 22, 23, 24, 25 and 26, located in the area of the perennial cold cyclonic eddy (Huang et al. 1992, Soong et al. 1995, Han 1998, Liao et al. 2006).
5. Stations 14, 15, 16, 17, 18, 19 and 20 are in the Luzon Strait for monitoring the KC passing through the Luzon Strait.
6. 32 monitoring stations are located in the northern SCS (Figure 1).

2.2. Sampling and analytical methods

Water samples were collected at all the above stations from 8 to 27 September 2006 from *Shiyan 3*, the research ship of the South China Sea Institute of Oceanology, Chinese Academy of Sciences. The sampling layers were designated according to the methods of ‘The specification for marine monitoring’ (GB17378-1998, China), and some stations were selected according to their depths. The depths included 0 m, 25 m, 50 m, 75 m, 100 m, 150 m, 200 m, 300 m, 400 m, 500 m, 600 m, 800 m, 1000 m, 1200 m,

1500 m, 2000 m, 2500 m, 3000 m and 3500 m. Water samples were analysed for nitrate ($\text{NO}_3\text{-N}$), nitrite ($\text{NO}_2\text{-N}$), ammonium ($\text{NH}_4\text{-N}$), silicate ($\text{SiO}_3\text{-Si}$), phosphorus ($\text{PO}_4\text{-P}$), dissolved oxygen (DO), chlorophyll *a* (Chl *a*), temperature (*T*), salinity (*S*), and pH (Wang et al. 2006, 2008, 2011). DO was determined using the Winkler titration method immediately on board. Temperature (*T*) and salinity (*S*) were measured with SBE911 plus Conductive Temperature Depth (CTD). The other samples were passed through $0.45\ \mu\text{m}$ GF/F filters, then poured into 500 ml LDPE bottles; following the addition of three drops of trichloromethane, the samples were deep-frozen immediately at -20°C . All the samples were analysed within two weeks of the end of this cruise. All the parameters were detected according to 'The specification for marine monitoring' (GB17378-1998, China).

2.3. Data analysis methods

The data sets consisted of 14 parameters for 32 stations, which contained different depths at different stations since the depths of the stations were different from each other. Only the following data sets were analysed: from the surface layers at all stations (Data1), from deep station 14 (Data2), and silicate from 0 m to 200 m of the stations which had homologous layers (Data3). The parameters selected included silicate ($\text{SiO}_3\text{-Si}$), nitrate ($\text{NO}_3\text{-N}$), nitrite ($\text{NO}_2\text{-N}$), ammonia ($\text{NH}_4\text{-N}$), phosphorus ($\text{PO}_4\text{-P}$), Temperature (*T*), Salinity (*S*), pH, dissolved oxygen (DO), chlorophyll *a* (Chl *a*), TIN, the ratio $\text{TIN}/\text{PO}_4\text{-P}$, the ratio of $\text{SiO}_3\text{-Si}/\text{PO}_4\text{-P}$ and the depth of stations (DP).

Initially, Data1 was used to show the surface distributions of every parameter, except DP, and to indicate the regions of upwelling. CA was then applied to cluster the stations into two groups to find which group was higher in nutrients; finally, PCA was used to analyse the parameters to identify the source of the nutrients and to decide which parameter could be used to reliably demonstrate regions of upwelling. Data2 and Data3 were selected to show the vertical and horizontal distributions of silicate, respectively, in order to show how upwelling was forming.

2.4. Multivariate statistical analysis methods

Data1 was processed using Multivariate statistical analysis methods, such as CA and PCA. CA is an unsupervised pattern detection method that partitions all cases into smaller groups or clusters of relatively similar cases that are dissimilar to other groups (Lattin et al. 2003, McKenna

2003, Wu & Wang 2007, Zhou et al. 2007). Hierarchical CA was used on standardized data, applying Ward's method with correlation. The low and high nutrient stations were determined from hierarchical CA using linkage distance.

PCA extracted eigenvalues and eigenvectors from the covariance matrix of the original variables, then produced new orthogonal variables known as PCs through VARIMAX rotation, which are linear combinations of the original variables. PCs provide information on the most meaningful parameters that describe a whole data set, allowing data reduction with minimum loss of original information. They are unobservable, hypothetical, latent variables (Vega et al. 1998, Helena et al. 2000, Pekey et al. 2004, Singh et al. 2004, Wu & Wang 2007, Zhou et al. 2007).

All the mathematical and statistical computations were performed using MATLAB R2008b (Mathworks Inc., USA) and ArcGIS 9.3 (ESRI Inc., USA).

2.5. Satellite data and image processing

MODIS-Aqua satellite images (4-km Level 3 HDF) covering the SCS were obtained from NASA. Weekly (8-day) composite sea surface temperature (SST) data from 14 to 21 September were used owing to the heavy cloud coverage around this region during the cruise. The SeaDAS package was used to process the SST imagery.

3. Results and discussion

3.1. Horizontal distribution of parameters

The horizontal distributions of parameter concentrations at the surface are shown in Figure 2. The horizontal distributions of surface $\text{NO}_2\text{-N}$ reveal that there are two high concentration regions: one is near the Pearl River Estuary in the north-west, the other is near the Luzon Strait in the south-east (Figure 2a). The $\text{NO}_3\text{-N}$ distribution shows four high nutrient regions: near the Pearl River, in the south-west, south-east and north-east of the PIS (Figure 2b). The $\text{NH}_4\text{-N}$ concentration is high in the north-west, north-east and south-east of the PIS (Figure 2c). $\text{SiO}_3\text{-Si}$ is distributed in three regions: (1) around and to the north-east of the PIS, (2) in the west of the PIS and (3) near the perennial cold cyclonic eddy (Figure 2d). The $\text{PO}_4\text{-P}$ distribution shows horizontal variations with increases from the southern to the northern regions; it is also found in the same three regions where silicate is distributed (Figure 2e). The distributions of DO and Chl *a* are

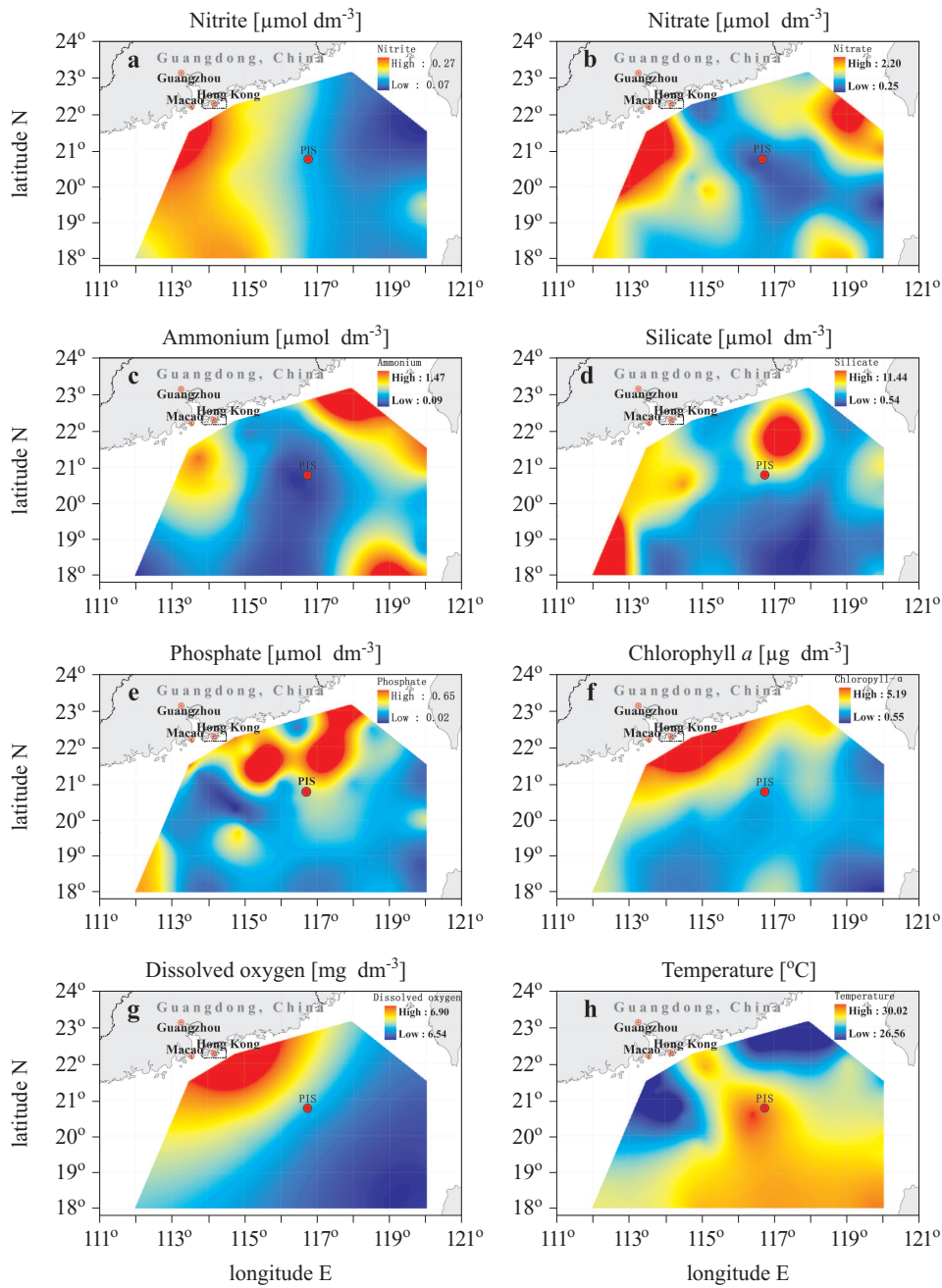


Figure 2. The distribution patterns of nitrite [$\mu\text{mol dm}^{-3}$] (a), nitrate [$\mu\text{mol dm}^{-3}$] (b), ammonium [$\mu\text{mol dm}^{-3}$] (c), silicate [$\mu\text{mol dm}^{-3}$] (d), phosphate [$\mu\text{mol dm}^{-3}$] (e), chlorophyll *a* [$\mu\text{g dm}^{-3}$] (f), dissolved oxygen [mg dm^{-3}] (g) and temperature [$^{\circ}\text{C}$] (h) at the surface in the northern SCS

similar: high near the coast and low in offshore waters. The offshore DO concentration is equal to 6.64 mol dm^{-3} . In contrast, Chl *a* shows three small, high-concentration regions in the Pearl River Estuary, the locations of which are similar to those of silicate (Figures 2f–g). The temperature distribution is significantly low in the north-east and the west of the PIS, and low at 114°E – 115°E in the south (Figure 2h).

The horizontal distributions of $\text{SiO}_3\text{-Si}$ and temperature show three upwelling regions: (1) the north-east of the PIS, (2) the west of the PIS and (3) the regions of the perennial cold cyclonic eddy.

3.2. Parameter distribution characteristics and data treatment

Before CA and PCA were performed, the normalization of the distribution of each variable was checked by kurtosis and skewness analysis (Johnson & Wichern 1992, Lattin et al. 2003, Papatheodorou et al. 2006, Zhou et al. 2007). The original data suggested that DP, $\text{NO}_3\text{-N}$, T and $\text{PO}_4\text{-P}$ were almost normally distributed, whereas the other parameters were positively skewed, with kurtosis coefficients significantly greater than three (95% confidence). After log-transformation of these other parameters (Kowalkowski et al. 2006, Zhou et al. 2007), all skewness and kurtosis values (except Chl *a*) were sharply reduced, ranging from -0.7742 to 0.5822 and from -0.7641 to 0.5840 , which were less than the critical values. For CA and PCA, all parameters were also z-scale standardized to minimize the effects of differences in measurement units and variance and to render the data dimensionless (Wu & Wang 2007, Zhou et al. 2007).

3.3. Spatial similarities and grouping at the monitoring stations

CA produced a dendrogram with two groups at $(\text{Dlink}/\text{Dmax}) \times 100 < 300$ (Figure 3). Group A consisted of stations 5, 7, 8, 13–17, 20–28, which is called the low nutrient group, and group B contained stations 1–4, 6, 9–12, 18, 19 and 29–32, called the high nutrient group. The classifications varied significantly, because the stations in these groups had similar features (low or high nutrient concentration), although these are caused by different natural backgrounds. The stations of the low nutrient group were far away from the mainland or the upwelling areas, whereas the stations of the high nutrient group came from the Pearl River Estuary (stations 1, 2, 3, 32, 31), or the upwelling regions (stations 4, 6, 9, 10, 11, 12 from the north-east of the PIS; 29, 30 from the upwelling region in the west of the PIS). Station 23 from the perennial cold cyclonic eddy region should be in the high nutrient group, but is in fact in the low nutrient group, since the upwelling driven by the perennial cold cyclonic eddy is not powerful enough at the surface (Wu 1991, Liao et al. 2006).

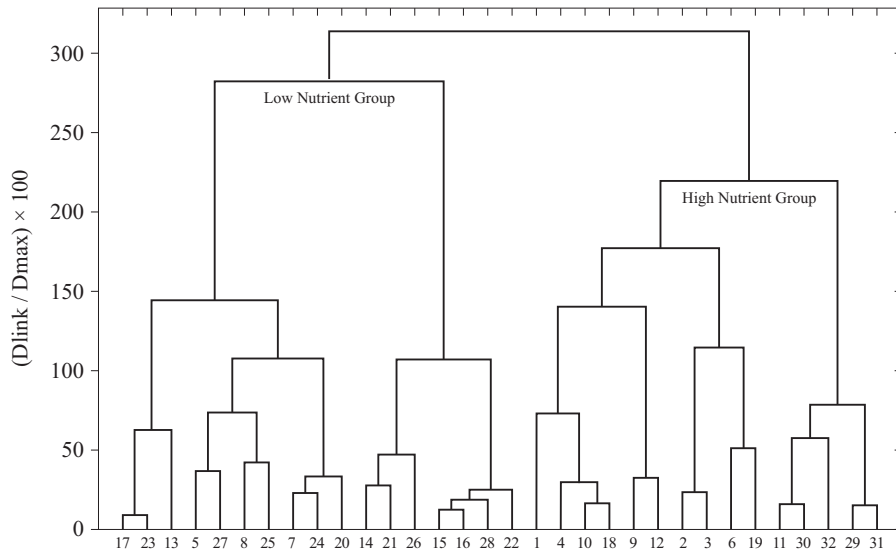


Figure 3. Results of Ward's method for cluster analysis showing two spatial clusters (low nutrient group and high nutrient group) of the monitoring stations

3.4. Source identification and indicator determination

Bartlett's sphericity test was performed on the parameter correlation matrix to examine the validity of the PCA (Wu & Wang 2007, Zhou et al. 2007). The significant level of Bartlett's sphericity test is 0 ($p < 0.05$), indicating that PCA may be useful in providing significant reductions in dimensionality.

PCA was conducted on standardized data sets of Data1 (z -scale standardized with mean and variance of zero and one, respectively) to analyse the source identification of nutrients (Mendiguchía et al. 2007, Zhou et al. 2007) and find the best indicator for upwelling formation. The linear correlation coefficients between the variables are shown in Table 1. As we expected, dissolved oxygen was strongly positively correlated with Chl a , which is a natural process because marine phytoplankton are the major oxygen producers here (Xu & Zhu 1999, Wu & Wang 2007).

Table 2 summarizes the PCA results comprising the loadings and eigenvalues. According to the eigenvalue-one criterion, the first five PCs with eigenvalues > 1 were considered essential. They explained 78.65% of the total variance. According to Table 2, the main contribution to PC1, explaining 27.64% of the total variance, was from TIN/PO₄-P. The ratios

Table 1. Linear correlation coefficients of 14 parameters (values in bold are significantly correlated at the $\alpha = 0.05$ significance level)

Parameter	NO ₂ -N	NO ₃ -N	NH ₄ -N	PO ₄ -P	SiO ₃ -Si	<i>T</i>	<i>S</i>	DO	pH	Chl <i>a</i>	TIN	TIN/ PO ₄ -P	SiO ₃ -Si/ PO ₄ -P	DP
NO ₂ -N	1.0000													
NO ₃ -N	-0.1435	1.0000												
NH ₄ -N	-0.1270	0.2183	1.0000											
PO ₄ -P	0.1653	-0.0630	-0.0274	1.0000										
SiO ₃ -Si	-0.1476	0.2511	0.2336	0.1378	1.0000									
<i>T</i>	-0.1181	-0.4171	-0.5180	0.1750	-0.2753	1.0000								
<i>S</i>	-0.2642	0.1459	0.1489	-0.3146	-0.0115	-0.2009	1.0000							
DO	0.1267	-0.1695	0.0353	0.1821	0.0868	0.0256	-0.5625	1.0000						
pH	-0.1553	-0.1172	0.2157	-0.2126	0.1547	-0.0637	-0.1537	0.3506	1.0000					
Chl <i>a</i>	0.3438	-0.0745	-0.0410	-0.0390	-0.1618	-0.3440	-0.2814	0.5171	0.1129	1.0000				
TIN	0.0759	0.6925	0.6661	-0.0606	0.2772	-0.6443	0.2565	-0.1675	-0.0668	0.0286	1.0000			
TIN/PO ₄ -P	-0.1025	0.3909	0.3480	-0.8735	0.0190	-0.4620	0.3906	-0.2354	0.1469	0.0469	0.5389	1.0000		
SiO ₃ -Si/PO ₄ -P	-0.2366	0.2484	0.2090	-0.5942	0.7148	-0.3471	0.2128	-0.0581	0.2757	-0.1038	0.2679	0.6321	1.0000	
DP	-0.2506	-0.1666	0.0438	-0.2233	-0.2404	0.4476	0.2933	-0.3060	-0.1889	-0.4729	-0.0764	0.1512	-0.0376	1.0000

Table 2. Loadings of 14 parameters on the first five PCs. The loadings whose absolute values are more than 0.4 are in bold, and the corresponding original variables are considered to contribute significantly to the PCs

Variables	PC1	PC2	PC3	PC4	PC5	PC6
NO ₂ -N	0.0843	-0.0627	0.3864	-0.1251	0.6604	-0.2968
NO ₃ -N	0.2731	0.2307	-0.4559	0.0241	0.4396	0.1462
NH ₄ -N	-0.2215	0.0346	-0.3971	-0.2348	0.0558	-0.5776
SiO ₃ -Si	-0.1658	0.0795	0.0848	-0.6196	-0.0542	0.5506
PO ₄ -P	0.3200	-0.0099	-0.3056	-0.6186	0.0727	-0.0635
DO	-0.0428	-0.6530	-0.1409	0.0637	0.1339	0.0762
Chl <i>a</i>	0.0395	-0.6025	-0.2681	0.0890	0.1328	0.2701
TIN	0.3474	0.1877	-0.4051	0.2522	-0.2675	0.0612
TIN/PO ₄ -P	-0.4727	0.1712	-0.3000	0.2064	0.3068	0.0501
SiO ₃ -Si/PO ₄ -P	-0.5700	0.1491	-0.1531	-0.0037	0.0997	0.2188
DP	0.2588	0.2429	0.1239	0.2097	0.3847	0.3419
eigenvalue	2.3665	2.0657	1.5885	1.4434	1.1461	1.0627
total variance (%)	21.5140	18.7790	14.4410	13.1220	10.4190	9.6613
cumulative variance (%)	21.5140	40.2930	54.7340	67.8560	78.2750	87.9363

of nitrogen to phosphorus are the key fraction of the Redfield ratio. PC1 represented nutrient limitation to phytoplankton growth in the study area. PC2, explaining 18.80% of the total variance, had positive loadings on DP, and negative loadings on DO and Chl *a*, which illustrated the similar features of the original data that DO and Chl *a* are high in coastal shallow stations and low in deep stations offshore (Figures 2f–g). PC3, explaining 12.97% of the total variance, had positive loadings on PO₄-P and negative loadings on pH. pH is determined mainly by biological activities, and PO₄-P comes mainly from the upwelling areas and the estuary in the northern SCS. PC3 therefore represented the impact of macronutrients on biological activities in the upwelling areas and the estuary. PC4, explaining 11.44% of the total variance, had negative loadings on SiO₃-Si. SiO₃-Si is replenished mainly by the upwelling from the deep sea in the northern SCS (Chen et al. 2001). PC4 represented the features of upwelling. PC5, explaining 7.81% of the total variance, had strong positive loadings on NH₄-N and represented the anthropogenic pollution near the Pearl River Estuary. The massive economic growth and urban development in the Pearl River Delta have resulted in excessive discharges of wastewater in the Pearl River Estuary. NH₄-N is an important indicator of anthropogenic pollution in the Pearl River Estuary.

3.5. Distribution pattern of silicate in the euphotic zone

Figure 4 shows the horizontal distribution patterns of silicate at different depths, including the surface, 50 m, 75 m, 100 m, 150 m and 200 m.

At the surface, the concentration of silicate is low ($< 3 \mu\text{mol dm}^{-3}$) in most of the northern SCS (Figure 4a). Three high concentration zones can be clearly distinguished: (1) the Taiwan Shoals upwelling in the north-east of the PIS showed a high concentration of $\sim 16.46 \mu\text{mol dm}^{-3}$; (2) the northern perennial cold cyclonic eddy in the south-west of the PIS had a relatively lower concentration of $\sim 5.29 \mu\text{mol dm}^{-3}$ at the centre; (3) the upwelling region in the west of the PIS was $\sim 11.96 \mu\text{mol dm}^{-3}$ (Figure 4a).

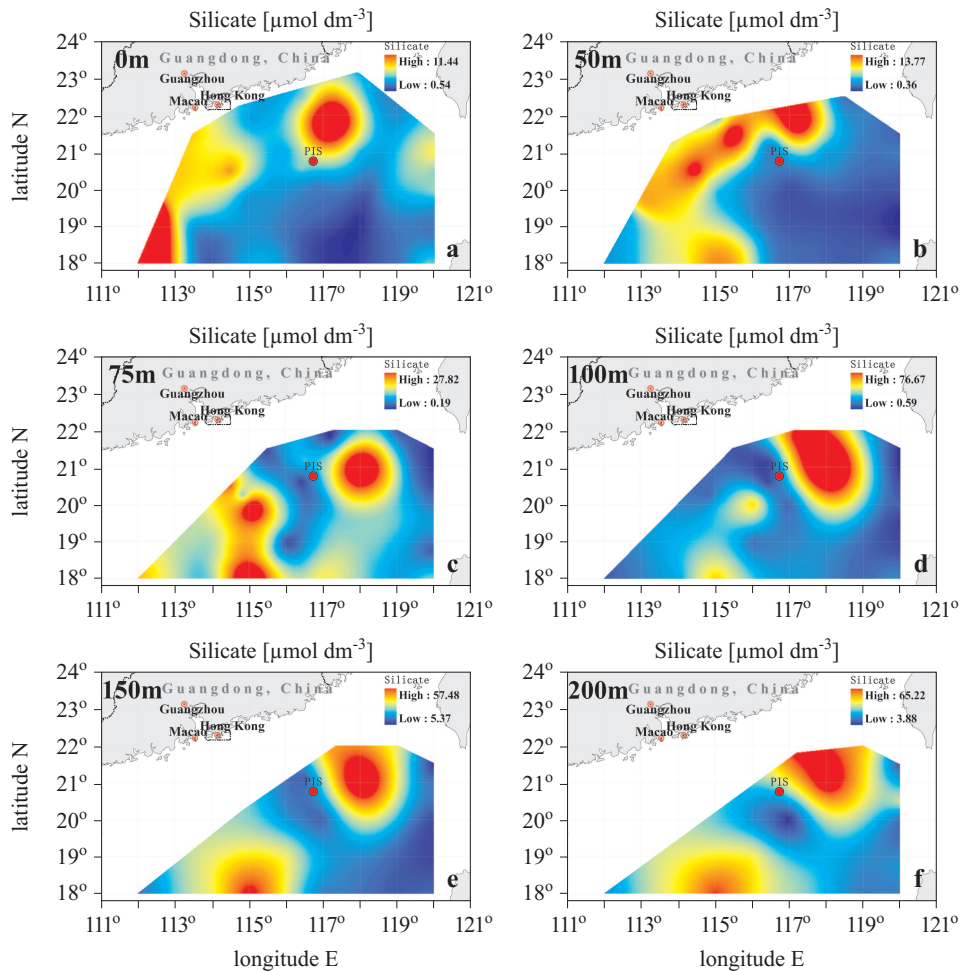


Figure 4. Distribution patterns of silicate in the 0 m (a), 50 m (b), 75 m (c), 100 m (d), 150 m (e) and 200 m (f) layers

The spatial distribution of silicate clearly shows three upwelling regions. In Figures 4a–f, the Taiwan Shoals upwelling has been formed at 200 m depth and is moving to the north-east, and its central concentration of silicate is decreasing from $65.3 \mu\text{mol dm}^{-3}$ to $16.46 \mu\text{mol dm}^{-3}$. These results illustrate that the Taiwan Shoals upwelling is formed by the deep-sea current climbing up the continental shelf near the PIS in a north-easterly direction. The northern part of the perennial cold cyclonic eddy is steady and stays at the same position in every layer, which is formed by the vertical uplifting current. The upwelling in the west of the PIS is detected at 100 m depth, and the horizontal distribution traces its process of formation. The upwelling in TSLS (Han 1998, Shen & Shi 2006) and in the perennial cold cyclonic eddy (Wu 1991, Huang et al. 1992, Soong et al. 1995, Liao et al. 2006) were determined by traditional methods from the low DO, temperature, high salinity or high chlorophyll *a* in the last decade.

3.6. The reliability and advantage of using silicate as an indicator of upwelling formation

Silicate availability may limit the growth of marine phytoplankton (Sakshaug et al. 1991, Yang et al. 2006). Yang et al. (2006) indicated that the Si concentration sufficient for phytoplankton growth ranged from $0.76 \mu\text{mol dm}^{-3}$ to $2.15 \mu\text{mol dm}^{-3}$ (mean $1.46 \mu\text{mol dm}^{-3}$) in Jiaozhou Bay of northern China. The diatom density varied from 5×10^5 to 6×10^6 cells m^{-3} in the northern SCS (Han 1998). Silicate concentrations in the upwelling centres at the surface were about $14.83 \mu\text{mol dm}^{-3}$, $11.53 \mu\text{mol dm}^{-3}$ and $5.29 \mu\text{mol dm}^{-3}$; these values are much higher than the $1.46 \mu\text{mol dm}^{-3}$ in Jiaozhou Bay (Yang et al. 2006). Therefore, silicate here may not be used up by phytoplankton in the upwelling centres.

Figure 5 shows that the silicate concentration at the bottom is 100 times higher than that at the surface: the deeper the station, the higher the concentration, such as station 14 located in the Luzon Strait (Figure 5).

The location of upwelling in the northern part of the SCS could be further verified by satellite observation of SST. Weekly composite SST images obtained during the cruise revealed a cooler area in the vicinity of the southern Taiwan Strait. The average SST within this block was about 1°C lower than the adjacent region to the south and south-east (Figure 6), indicating the existence of an apparent upwelling event.

Dissolved oxygen (DO), temperature, salinity and chlorophyll are the main indicators in studying upwelling in the northern SCS (Tang et al. 1999, Chen et al. 2004). Generally, it is difficult to apply these indicators to identify upwelling events since many additional factors may weaken them as useful indicators. Precipitation and evaporation will affect salinity,

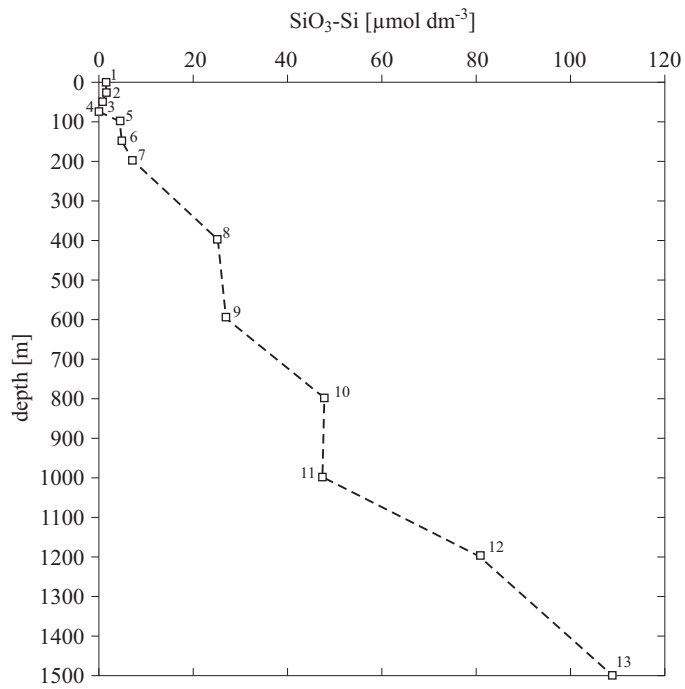


Figure 5. Vertical distribution of silicate concentration at different depths at station 14

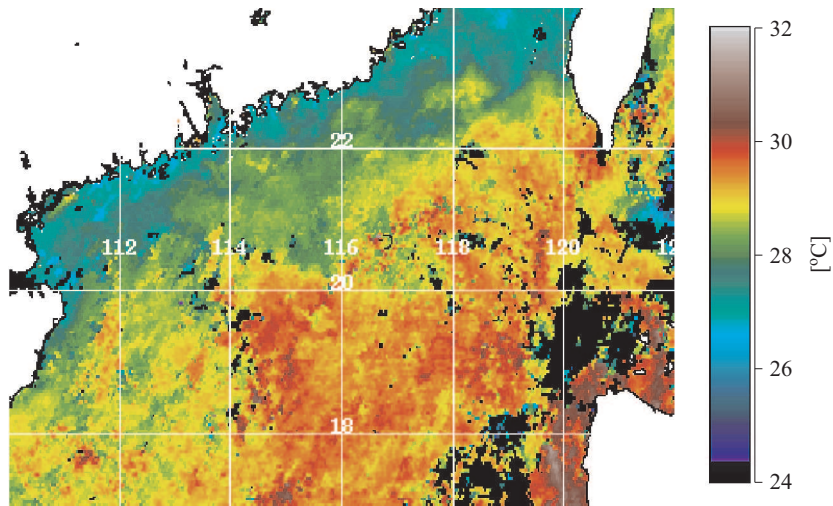


Figure 6. Satellite image of 8-day composite SST (14–21 Sept. 2006)

and the sea-air heat exchange affects temperature. DO turns out to be saturated, owing to the photosynthesis of the abundant phytoplankton in

the upwelling region. Most of the phytoplankton is consumed by marine grazers, leaving little chlorophyll in the upwelling waters (Chen et al. 2004). The offshore $\text{SiO}_3\text{-Si}$ comes mainly from replenishment by upwelling in the northern SCS, and nitrogen from regeneration and N_2 -fixation (Wu et al. 2003). The concentration of $\text{PO}_4\text{-P}$ is always one order of magnitude lower than that of $\text{SiO}_3\text{-Si}$ (Chen et al. 2004). Therefore, it is essential to confirm $\text{SiO}_3\text{-Si}$ as an indicator for upwelling research in the northern SCS.

One limitation to the application of the $\text{SiO}_3\text{-Si}$ indicator for upwelling is that if the upwelling is weak, $\text{SiO}_3\text{-Si}$ may be depleted by the phytoplankton at the surface. In nutrient-limited surface ocean waters, the export production of silicon is controlled largely by the input of $\text{SiO}_3\text{-Si}$, whereas the export production of nitrogen can also be controlled by grazing rate and regeneration (Dugdale et al. 1995, Hutchins & Bruland 1998). Once the nitrogen replenished by upwelling is depleted by the phytoplankton bloom, it can be replenished by other pathways such as N_2 -fixation and regeneration by abundant grazers. If the input rate of $\text{SiO}_3\text{-Si}$ is lower than the export rate, $\text{SiO}_3\text{-Si}$ will eventually be depleted by diatom uptake. It is clear from Figure 4a that the $\text{SiO}_3\text{-Si}$ concentration in the northern part of the cold eddy was so low that it could not markedly indicate the upwelling. The $\text{SiO}_3\text{-Si}$ at the centres of the upwellings in the TSLs and in the west of the PIS was not depleted by diatoms. This confirmed that the upwelling in the TSLs and the upwelling in the west of the PIS were stronger than that in the northern part of the cold eddy, with the one in the TSLs being the strongest.

4. Conclusions

With the aid of multivariate statistical analysis and remote sensing techniques, we successfully demonstrated that silicate is a useful indicator of the formation and distribution of upwelling events in the northern part of the SCS, especially for the analysis and interpretation of complex data from large areas, such as for marine environmental and ecological research (Wang et al. 2006, Chau & Muttill 2007, Suikkanen et al. 2007, Wu & Wang 2007, Wu et al. 2009a,b). Although the complex datasets used here consist of 32×14 observations in a large area ($18^\circ\text{--}23^\circ\text{N}$, $111^\circ\text{--}120^\circ\text{E}$), the CA clearly distinguished the spatial similarity reflecting different levels of nutrient concentration (low and high nutrient), and the PCA was successful in picking out silicate as an indicator for studying upwelling. The spatial distribution of silicate clearly showed three upwelling regions that can be verified by satellite observations of sea surface temperature.

References

- Chau K. W., Muttill N., 2007, *Data mining and multivariate statistical analysis for ecological system in coastal waters*, J. Hydroinform., 9(4), 305–317, doi:10.2166/hydro.2007.003.
- Chen C. C., Shiah F. K., Chung S. W., Liu, K. K., 2006, *Winter phytoplankton blooms in the shallow mixed layer of the South China Sea enhanced by upwelling*, J. Marine Syst., 59(1–2), 97–110, doi:10.1016/j.jmarsys.2005.09.002.
- Chen C.-T. A., Hsing L.-Y., Liu, C.-L., Wang S.-L., 2004, *Degree of nutrient consumption of upwelled water in the Taiwan Strait based on dissolved organic phosphorus or nitrogen*, Mar. Chem., 87(3–4), 73–86, doi:10.1016/j.marchem.2004.01.006.
- Chen C.-T. A., Huang, M.-H., 1996, *A mid-depth front separating the South China sea water and the Philippine sea water*, J. Oceanogr., 52(1), 17–25, doi:10.1007/BF02236530.
- Chen C.-T. A., Wang S.-L., Wang B.-J., Pai S.-C., 2001, *Nutrient budgets for the South China Sea basin*, Mar. Chem., 75(4), 281–300, doi:10.1016/S0304-4203(01)00041-X.
- Chen S. T., Ruan W. Q., 1991, *Summer upwelling and saturation dissolved oxygen distribution in the Central and Northern Taiwan Strait*, Chinese J. Oceanogr. Taiwan Strait, 10(1), 16–24, (in Chinese).
- Di Lorenzo E., 2003, *Seasonal dynamics of the surface circulation in the Southern California Current System*, Deep-Sea Res. Pt. II, 50(14–16), 2371–2388, doi:10.1016/S0967-0645(03)00125-5.
- Dugdale R. C., Wilkerson F. P., Minas H. J., 1995, *The role of a silicate pump in driving new production*, Deep-Sea Res. Pt. I, 42(5), 697–719, doi:10.1016/0967-0637(95)00015-X.
- Han W. Y., 1998, *Marine chemistry in the South China Sea*, Science Press, Beijing, 298 pp., (in Chinese).
- Helena B., Pardo R., Vega M., Barrado E., Fernandez J. M., Fernandez L., 2000, *Temporal evolution of groundwater composition in an alluvial aquifer (Pisuerga River, Spain) by principal component analysis*, Water Res., 34(3), 807–816, doi:10.1016/S0043-1354(99)00225-0.
- Hong Q. M., Li L., 1991, *A study of upwelling over continental shelf off eastern Guangdong*, Chinese J. Oceanogr. Taiwan Strait, 10(3), 271–277, (in Chinese).
- Hu J. Y., Liu M. S., 1992, *The current structure during summer in southern Taiwan Strait*, Chinese J. Tropical Oceanogr., 11(4), 42–47, (in Chinese).
- Huang Q. Z., Wang W. Z., Li Y. S., Li C. W., Mao M., 1992, *General situation of the current and eddy in the South China Sea*, Chinese J. Adv. Earth Sci., 5, 1–9, (in Chinese).
- Hutchins D. A., Bruland K. W., 1998, *Iron-limited diatom growth and Si:N uptake ratios in a coastal upwelling regime*, Nature, 393(6685), 561–564, doi:10.1038/31203.

- Johnson R. A., Wichern D. W., 1992, *Applied multivariate statistical analysis*, 5th edn., Prentice-hall, New Jersey.
- Kowalkowski T., Zbytniewski R., Szpejna J., Buszewski B., 2006, *Application of chemometrics in river water classification*, *Water Res.*, 40 (4), 744–752, doi:10.1016/j.watres.2005.11.042.
- Latin J., Carroll D., Green P., 2003, *Analyzing multivariate data*, Duxbury Press, New York, 580 pp.
- Liao G. H., Yuan Y. C., Wang Z. G., 2006, *The three dimensional structure of the circulation in the South China Sea during the summer of 1998*, *Acta Oceanol. Sin.*, 28 (5), 15–25.
- Liu K.-K., Chao S.-Y., Shaw P.-T., Gong G.-C., Chen C.-C., Tang T. Y., 2002, *Monsoon-forced chlorophyll distribution and primary production in the South China Sea: observations and a numerical study*, *Deep-Sea Res. Pt. I*, 49 (8), 1387–1412, doi:10.1016/S0967-0637(02)00035-3.
- McKenna J. E., 2003, *An enhanced cluster analysis program with bootstrap significance testing for ecological community analysis*, *Environ. Modell. Softw.*, 18 (3), 205–220, doi:10.1016/S1364-8152(02)00094-4.
- Mendiguchía C., Moreno C., García-Vargas M., 2007, *Evaluation of natural and anthropogenic influences on the Guadalquivir River (Spain) by dissolved heavy metals and nutrients*, *Chemosphere*, 69 (10), 1509–1517.
- Mohtadi M., Hebbeln D., Marchant M., 2005, *Upwelling and productivity along the Peru-Chile Current derived from faunal and isotopic compositions of planktic foraminifera in surface sediments*, *Mar. Geol.*, 216 (3), 107–126, doi:10.1016/j.margeo.2005.01.008.
- Monteiro P. M. S., Largier J. L., 1999, *Thermal stratification in Saldanha Bay (South Africa) and subtidal, density-driven exchange with the coastal waters of the Benguela upwelling system*, *Estuar. Coast. Shelf Sci.*, 49 (6), 877–890, doi:10.1006/ecss.1999.0550.
- Morton B., Blackmore G., 2000, *South China Sea*, *Mar. Pollut. Bull.*, 42 (12), 1236–1263, doi:10.1016/S0025-326X(01)00240-5.
- Nixon S., Thomas A., 2001, *On the size of the Peru upwelling ecosystem*, *Deep-Sea Res. Pt. I*, 48 (11), 2521–2528, doi:10.1016/S0967-0637(01)00023-1.
- Papatheodorou G., Demopoulou G., Lambrakis N., 2006, *A long-term study of temporal hydrochemical data in a shallow lake using multivariate statistical techniques*, *Ecol. Model.*, 193 (3–4), 759–776, doi:10.1016/j.ecolmodel.2005.09.004.
- Pekey H., Karakaş D., Bakoğlu M., 2004, *Source apportionment of trace metals in surface waters of a polluted stream using multivariate statistical analyses*, *Mar. Pollut. Bull.*, 49, 809–818, doi:10.1016/j.marpolbul.2004.06.029.
- Pelegrí J. L., Marrero-Díaz A., Ratsimandresy A., Antoranz A., Cisneros-Aguirre J., Gordo C., Grisolia D., Hernández-Guerra A., Láiz I., Martínez A., Parrilla G., Pérez-Rodríguez P., Rodríguez-Santana A., Sangrà P., 2005, *Hydrographic cruises off northwest Africa: the Canary Current and the Cape Ghir region*, *J. Marine Syst.*, 54 (1–4), 39–63, doi:10.1016/j.jmarsys.2004.07.001.

- Prego R., Guzmán-Zuñiga D., Varela M., de Castro M., Gómez-Gesteira M., 2007, *Consequences of winter upwelling events on biogeochemical and phytoplankton patterns in a western Galician ria (NW Iberian peninsula)*, Estuar. Coast. Shelf Sci., 73 (3–4), 409–422, doi:10.1016/j.ecss.2007.02.004.
- Sakshaug E., Slagstad D., Holm-Hansen O., 1991, *Factors controlling the development of phytoplankton blooms in the Antarctic Ocean – a mathematical model*, Mar. Chem., 35 (1–4), 259–271, doi:10.1016/S0304-4203(09)90021-4.
- Shen G. Y., Shi B. Z., 2006, *Marine Ecology*, Sci. Press, Beijing, (in Chinese).
- Shrestha S., Kazama F., 2007, *Assessment of surface water quality using multivariate statistical techniques: a case study of the Fuji river basin, Japan*, Environ. Modell. Softw., 22 (4), 464–475, doi:10.1016/j.envsoft.2006.02.001.
- Singh K.P., Malik A., Mohan D., Sinha S., 2004, *Multivariate statistical techniques for the evaluation of spatial and temporal variations in water quality of Gomti River (India) – a case study*, Water Res., 38 (18), 3980–3992, doi:10.1016/j.watres.2004.06.011.
- Soong Y. S., Hu J.-H., Ho C.-R., Niiler P. P., 1995, *Cold-core eddy detected in South China Sea*, EOS Trans. AGU, 76 (35), 345–345, doi:10.1029/95EO00209.
- Su J.L., Wang W., 1990, *On the sources of Taiwan Warm current from South China Sea*, Chinese J. Donghai Mar. Sci., 8 (3), 1–9, (in Chinese).
- Suikkanen S., Laamanen M., Huttunen M., 2007, *Long-term changes in summer phytoplankton communities of the open northern Baltic Sea*, Estuar. Coast. Shelf Sci., 71 (3–4), 580–592, doi:10.1016/j.ecss.2006.09.004.
- Tang D. L., Kester D. R., Ni I.-H., Kawamura H., Hong H.-S., 2002, *Upwelling in the Taiwan Strait during the summer monsoon detected by satellite and shipboard measurements*, Remote Sens. Environ., 83 (3), 457–471, doi:10.1016/S0034-4257(02)00062-7.
- Tang D.L., Ni I.-H., Kester D.R., Müller-Karger F.E., 1999, *Remote sensing observations of winter phytoplankton blooms southwest of the Luzon Strait in the South China Sea*, Mar. Ecol.-Prog. Ser., 191, 43–51, doi:10.3354/meps191043.
- Traganza E. D., Nestor D. A., McDonald A. K., 1980, *Satellite observations of a nutrient upwelling off the coast of California*, J. Geophys. Res., 85 (C7), 4101–4106, doi:10.1029/JC085iC07p04101.
- Vega M., Pardo R., Barrado E., Deban L., 1998, *Assessment of seasonal and polluting effects on the quality of river water by exploratory data analysis*, Water Res., 32 (12), 3581–3592, doi:10.1016/S0043-1354(98)00138-9.
- Wang Y. S., Lou Z. P., Sun C. C., Sun S., 2008, *Ecological environment changes in Daya Bay, China, from 1982 to 2004*, Mar. Pollut. Bull., 56 (11), 1871–1879, doi:10.1016/j.marpolbul.2008.07.017.
- Wang Y.-S., Lou Z.-P., Sun C.-C., Wu M.-L., Han S.-H., 2006, *Multivariate statistical analysis of water quality and phytoplankton characteristics in Daya Bay, China, from 1999 to 2002*, Oceanologia, 48 (2), 193–211.

- Wang Y.-S., Sun C.-C., Lou Z.-P., Wang H., Mitchell B.G., Wu M.-L., Sun Z.-X., 2011, *Identification of water quality and benthos characteristics in Daya Bay, China, from 2001 to 2004*, *Oceanol. Hydrobiol. St.*, 40 (1), 82–95, doi:10.2478/s13545-011-0009-4.
- Woodson C.B., Eerkes-Medrano D.I., Flores-Morales A., Foley M.M., Henkel S.K., Hession-Lewis M., Jacinto D., Needles L., Nishizaki M.T., O’Leary J., Ostrand C.E., Pespeni M., Schwager K.B., Tyburczy J.A., Weersing K.A., Kirincich A.R., Barth J.A., McManus M.A., Washburn L., 2007, *Local diurnal upwelling driven by sea breezes in northern Monterey Bay*, *Cont. Shelf Research*, 27 (18), 2289–2302, doi:10.1016/j.csr.2007.05.014.
- Wu L.X., 1991, *Physical chemical characteristics of seawater in the cold eddy southwest of Dongsha Islands*, *Chinese J. Tropical Oceanol.*, 10 (4), 37–43, (in Chinese).
- Wu M.-L., Wang Y.-S., 2007, *Using chemometrics to evaluate anthropogenic effects in Daya Bay, China*, *Estuar. Coast. Shelf Sci.*, 72 (4), 732–742, doi:10.1016/j.ecss.2006.11.032.
- Wu M.-L., Wang Y.-S., Sun C.-C., Wang H., Lou Z.-P., Dong J.-D., 2009a, *Using chemometrics to identify water quality in Daya Bay, China*, *Oceanologia*, 51 (2), 217–232.
- Wu M.-L., Wang Y.-S., Sun C.-C., Wang H., Dong J.-D., Han S.-H., 2009b, *Identification of anthropogenic effects and seasonality on water quality in Daya Bay, South China Sea*, *J. Environ. Manage.*, 90 (10), 3082–3090, doi:10.1016/j.jenvman.2009.04.017.
- Wu R.S., Li L., 2003, *Summarization of study on upwelling system in the South China Sea*, *Chinese J. Oceanogr. Taiwan Strait*, 22 (2), 269–277, (in Chinese).
- Xu C., Zhu Z.H., 1999, *pH, alkalinity and dissolved oxygen*, [in:] *Researches on Ecosystem of Daya Bay*, Q. Jin (ed.), China Meteorol. Press, Beijing, China, 13–24, (in Chinese).
- Yang D.F., Gao Z.H., Sun P.Y., 2006, *Mechanism of nutrient silicon and water temperature influences on phytoplankton growth*, *Chinese J. Mar. Sci. Bull.*, 8, 49–59, (in Chinese).
- Zhou F., Guo H.C., Liu Y., Jiang Y.M., 2007, *Chemometrics data analysis of marine water quality and source identification in Southern Hong Kong*, *Mar. Pollut. Bull.*, 54 (6), 745–756, doi:10.1016/j.marpolbul.2007.01.006.